N87-22348

TURBULENCE AS OBSERVED BY CONCURRENT MEASUREMENTS MADE AT NSSL USING WEATHER RADAR, DOPPLER RADAR, DOPPLER LIDAR, AND AIRCRAFT

Jean T. Lee
National Severe Storms Laboratory
Norman, Oklahoma

ABSTRACT

As air traffic increases and aircraft capability increase as to range and operating altitude, the exposure to weather hazards increases. Turbulence and wind shears are two of the most important of these hazards that must be taken into account if safe flight operations are to be accomplished.

Beginning in the early 1960's, Project Rough Rider began thunderstorm investigations. This paper summarizes past and present efforts at the National Severe Storm Laboratory (NSSL) to measure these flight safety hazards and to describe the use of Doppler radar to detect and quantify these hazards. In particular, the evolution of the Doppler-measured radial velocity spectrum width and its applicability to the problem of safe flight is presented.

1. INTRODUCTION

Quantative data presentation and information assimilation are becoming increasingly important as Doppler radar evolves toward operational use by the weather services. Weather radar researchers have been faced with the development of techniques to identify and measure wind shear, vortices, and turbulence which constitute weather hazards to aviation. This paper summarizes past and present efforts at the NSSL in regards to weather hazards in convective cloud areas which can be encountered in aircraft operation.

2. BACKGROUND

Modern concepts of the internal structure of thunderstorms are developing mainly from multiple Doppler radar observations. Used in combinations of two or more, these radars now provide detailed portrayals of the precipitation-traced airflow in and beneath storm clouds and give new insights regarding the location of severe weather events. Furthermore, we can expect to see Doppler radar applications extended to include practical methods for measuring wind fields in optically clear air outside of storms for various altitudes [1]. The intensity of the radar return has been and still is used routinely by many to identify and track areas of heavy precipitation and hail (for examples see [2,3,4]), and operational tests have shown the great value of the radial velocity data in detecting mesocyclones and predicting tornadoes [5].

Thus, Doppler radar technology offers the unique opportunity to watch the complete development cycle of thunderstorms with a proven capability for

* C-2

early detection of aviation hazards and other severe weather events, and a likely capability to anticipate the rapid intensification which precedes severity [6].

The rationale for developing new diagnostic procedures is that:

1. Warnings will depend on real-time detection of singular events which provide controllers with criteria for advising pilots where dangerous conditions exist, and

2. Forecasts of severe weather events will depend on pattern recognition techniques which will provide aviation meteorologists, pilots, and air traffic personnel with criteria for predicting the likelihood (and locations) of hazardous weather events for flight and control planning.

Computer software to produce both types of products quickly and accurately depend on research studies which: (1) Objectively define data requirements, and (2) establish relationships among reflectivity, radial mean velocity, and spectral width with known weather hazards. Although this has been done and tested for mesocyclones and tornadoes, and to some extent for heavy rain and hail, work remains to better define the boundaries for turbulence, dangerous shear, strong directional outflow (gust fronts), and microburst.

2. HISTORY

The thunderstorm project of 1946 and 1947 was the first systematic documentation of these hazards at flight levels below 25,000 ft. In the 1950's, United Air Lines conducted studies in conjunction with commercial flights over the midwestern United States. With the advent of commercial jet aircraft operations at altitudes to 40,000 ft and increased air traffic density, accidents, and incidents involving aircraft in the vicinity of thunderstorms it was determined that a greater understanding of the thunderstorm was required. While a simple detour of all convective storms is the easiest way to avoid the associated hazards, the economics of civil aviation operations and non-combat military flights require a minimum disruption of service while safety is not compromised. Since the early 1960's, a cooperative research program involving the Federal Aviation Administration (FAA), National Aeronautics and Space Administration (NASA), U.S. Air Force (USAF), National Research Council (NRC) of Canada, the Royal Aircraft Establishment (RAE) at Bedford, England, and NSSL of the National Oceanographic and Atmospheric Administration (NOAA) has been in operation in Oklahoma. From 1960 to 1982 aircraft made controlled flights into thunderstorms of varying intensities (Figure 1) in order to determine the distribution of the hazards and their possible correlation with observations made by indirect probes such as weather radar and later with Doppler weather radar and lidars. In fact, we now recognize that radar correctly used and interpreted provides the best method known to date to improve the safety of flight near thunderstorms.

3. TURBULENCE

In the pre-Doppler era, over 500 penetrations of thunderstorms were made above 20,000 ft and a representative sample was obtained. In a second phase following the completion of the first phase, aircraft flights were confined to lower altitudes to obtain a sufficient sample size.

All aircraft were instrumented to measure and record the time, duration, and magnitude of the turbulence encountered during flight as well as other pertinent flight parameters. From these readings, derived gust velocities were calculated. The derived gust velocities are proportional to the change in acceleration (ΔN). The aircraft were tracked by the radar at Norman, and the position of the aircraft and the thunderstorm echo displayed on a Plan Position Indicator (PPI) scope were photographically recorded (Figure 2).

It was found early in the flight program that reflectivities of 10^5 mm^6m^{-3} (50 dBZ) were often associated with 3/4-inch diameter hail or layers [7], sizes that cause damage to an aircraft. Therefore, areas of indicated hail were avoided, and it may be possible that the gust velocities in these areas (Z_e values $\geq 10^5$ mm^6m^{-3}) exceed those measured outside of the area. Figures 3 and 4 are graphs of the distance from the center of the storm core when encounters of turbulence having derived gust velocities equal to or greater than 20 ft sec^{-1} were recorded. Storms of greater intensity were associated with greater gust velocities and with greater distances of significant turbulence from storm centers [8]. If one considers the average diameter of a severe thunderstorm to be 10 to 15 miles--a radius of 5 to 7.5 miles--it is apparent that severe turbulence can be encountered even near the edge of the visible cloud.

I would like to quote one conclusion from a report* by the National Research Council of Canada on flights conducted in Oklahoma:

> The results of this experiment are considered extremely important from an operational standpoint. It has been shown that at lower levels around squall lines and thunderstorms the return from weather radar provides insufficient information for avoidance of moderate and often severe turbulence, unless the aircraft is maneuvered in such a way as to avoid all radar echo by well over five miles. The intensity of turbulence encountered at this distance lends support to the view that echoes should be avoided by at least 10 miles and possibly more.

This view of turbulence differs from that of hail; the latter is closely related to echo intensity in a particular area because hailstones are themselves strong radar targets. At this time in our research we think of a thunderstorm system as a cluster of cells. The maximum radar reflectivity of which is an indicator of overall storm intensity, with the overall intensity determining the probability of hazardous turbulence, and the location of hail specifically indicated by the strong echo centers.

The two sampling phases (high and low altitude) produced similar statistics (Figure 5) which can be interpreted as meaning that turbulence

*G. K. Mather and D. S. Treddenick: Turbulence Measurements at Low Levels Around Squall Lines, National Research Council of Canada Aeronautical Report LR-515, 1969.

encounters vary little with altitude. These sample penetrations also showed that turbulence could be related to radar reflectivity only in the broadest sense and that such a measure as reflectivity gradient was not the answer and, in fact, could be very misleading.

The next major stride was made when Doppler radar was applied to observe meteorological phenomena. Doppler radar offers the highest potential for further defining turbulence because turbulence is known to be related kinematically to features that are best measured remotely with a Doppler radar.

4. DOPPLER RADAR AND TURBULENCE

The NSSL staff began a series of experiments in 1973 using the Doppler radar in place of the conventional WSR-57 weather radar to study weather hazards to aviation. These joint experiments involved the USAF, FAA, NASA, Colorado State University, University of Oklahoma, and various NOAA components. Penetration aircraft (F-4-C, F-101, F-100, and F-106) suitably equipped to make in situ wind and turbulence measurements, were used simultaneously with the Doppler radar.

One of the first experiments used the Plan Shear Indicator (PSI) developed by the USAF Cambridge Research Laboratory (now known as the Air Force Geophysical Laboratory (AFGL); this device graphically depicts radial shear [9] (Figure 6).

Moderate or severe turbulence was encountered in all cases when the PSI displayed shear along the aircraft flight path, but shear was not indicated with all turbulence encounters, and it appears from these cases that moderate or less turbulence (derived gust velocities (U_{de}) $\leq$ 9.1 ms^{-1}) may escape detection by the PSI. This is not surprising since only the wind's radial component is measured by radar. Where severe turbulence (U_{de} > 9.1 ms^{-1}) repeatedly was encountered, the PSI showed transient shear areas along the flight path. Arc deformations apparently have an operational detectability threshold associated with wind shears $\geq 1.5 \times 10^{-2}s^{-1}$.

In 1974, a second-generation radar real-time display was developed at NSSL. The three spectral moments were presented as a field of arrows shown by a minicomputer-graphic display terminal interfaced to the NSSL Doppler radar [10]. Arrow length is proportional to the logarithm of received power, arrow direction displacement from a horizontal position is proportional to velocity (similar to a speedometer indicator) and the arrowhead size to Doppler spectrum width (Figure 7).

Using the new display for real-time analysis, we directed USAF Aeronautical System Command F-4-C aircraft in a number of thunderstorm penetrations, and successfully located areas where the aircraft experienced turbulence. In post-analysis, the data were searched for significant correlations between turbulence, radar reflectivity, and velocity data. Figure 8 is a time history of aircraft-recorded turbulence and Doppler velocity spectrum width along the flight path. Note how well the turbulence trend matches the trend in the spectrum width plot. A total of 45 such penetrations were analyzed; all show a similar relationship. During the 45 penetrations, there were 76 occurrences of moderate or greater turbulence. Ninety-five percent had spectrum widths of 4.0 ms^{-1} or greater [11]. There will be non-turbulent areas where the spectral width is large because the spectral width may be biased by wind shear and beam broadening [12]. However, in two tornadic storms studied, the cumulative probability for the spectrum width to be ≥ 4 ms^{-1} due to all factors is only about 30 percent [13]. For non-severe storms the probability is even less; thus, only a small portion of even a severe storm will have "false alarm" values.

In another set of experiments analyzed by Bohne [14], a correlation of 0.89 was obtained between the curves showing turbulence measured by aircraft and radar along a flight path. More importantly, for higher turbulence levels, which pose a greater flight hazard, the agreement between radar measurements and the turbulence actually experienced by the aircraft was nearly total. Other experiments have led to similar conclusions [15]. Judging from available information, it appears that a spectrum width threshold of 4 ms^{-1} may be associated with the onset of flight discomfort and 6 ms^{-1} with potential hazard. The Next Generation Radar (NEXRAD) is expected to estimate Doppler spectrum widths with an accuracy of 1 ms^{-1} down to a signal-to-noise ratio (SNR) of 5 dB [16]. For a radar of the NEXRAD type, this means that good estimates of spectrum width (turbulence) can be obtained out to the maximum range of 230 km even with very light precipitation, of the order of 0.3 mm hr^{-1}.

Aircraft penetration studies have further shown that extreme turbulence may occur as far as 20 nautical miles (36 km) from the edge of the radar contour of the center of severe thunderstorm clouds, and the FAA advises pilots to avoid all thunderstorms by a margin at least equal to this distance [17]. This is a safe procedure to follow in relatively uncrowded airspace. In airlanes with heavy traffic, however, it is desirable to keep detours to a minimum. NEXRAD can help in this content in two main ways. First, since it can accurately sense precipitation and turbulence, it can better define the boundaries of thunderstorms. Thus, uncertainties due to impressive edge definition will be minimized. Second, unlike present operational weather and ATC radars which scan the azimuth with fixed antenna elevations, NEXRAD will scann its surrounding space at several elevation angles providing a three-dimensional picture of storms. Thus, flights well above the tops of thunderstorms may not have to be disturbed.

In addition, turbulence appears to be nearly isotropic and therefore independent of viewing angle. Figure 9 shows a comparison of the spectrum widths in a storm being observed by both Norman and Cimerron radars which are separated by more than 40 km. We have looked at several storms with four to six elevations per case and have found essentially the same result. This also tends to substantiate the findings of isotrophicity in the turbulence data gathered during earlier penetration flights.

We have also looked at comparing Doppler-radar-measured turbulence with that measured by Doppler lidar and by a 444 m (1500 ft) instrumented KTVY-TV tower. Figure 10 shows the agreement in wind speed and direction and Figure

11 the comparison of the standard deviations (turbulence) of the horizontal velocity fluctuations [18]. The variances of the u and v components were computed for each lidar- and radar-estimated vector wind field and combined to find $\sigma_T = (\sigma_u^2 + \sigma_v^2)^{1/2}$, the standard deviation of the horizontal velocity fluctuations. The total variance is taken as being composed of the errors due to velocity estimates and that due to turbulence and small-scale flows. It can be seen that the horizontal velocity fluctuations measured by the three different systems is in remarkable agreement.

It also appears that turbulent areas in a storm are not randomly distributed (Figure 12). Figures 13 and 14 show how a NEXRAD algorithm of turbulence and a smoothing integration produces turbulent areas (volumes) which can be tracked in time and space thus making the output valuable for the aviation community.

Wind shear such as seen in gust fronts and downbursts are also amenable to Doppler radar use in their detection. However, there remains to be accomplished the numerical modeling of these features to determine if their formation, movement, and intensification (or decay) can be accurately predicted and this is the area in which NSSL is now engaged.

5. SUMMARY

Turbulence, wind shear, microburst, and hail are amenable to observation by Doppler radar. Techniques to obtain the information and present the probabilities of encounter in an effective manner is a goal of the NEXRAD system. Emphasis at NSSL has now shifted from aircraft in situ measurements to the corresponding remote sensor observation and the modeling of these hazards for use in the NEXRAD environment and in aircraft operations.

6. REFERENCES

1. Berger, M. I.; and Doviak, R. J.: An Analysis of the Clear Air Planetary Boundary Layer Wind Synthesized from NSSL's Dual Doppler Radar Data. NOAA Technical Memo. ERL NSSL-87, 1979, 55 pp.

2. Zittel, W. D.: Evaluation of a Remote Weather Radar Display, Vol. II Computer Applications for Storm Tracking and Warning. FAA Report No. FAA-RD-75-60, 1976, 114 pp.

3. Elvander, R. C.: An Evaluation of the Relative Performance of Three Weather Radar Echo Forecasting Techniques. *Preprints: 17th Radar Meteorology Conference*, Seattle, Washington, 1976. American Meteorological Society, pp. 526-532.

4. Bjerkaas, C. L.; and Donaldson, R. J.: Real Time Tornado Warning Utilizing Doppler Velocities from a Color Display. *Preprints: 18th Radar Meteorology Conference*, Atlanta, Ga., 1978. American Meteorological Society, pp. 449-452.

5. National Oceanographic and Atmospheric Administration (NOAA): Final Report on the Joint Doppler Operational Project (JDOP) 1976-1978. NOAA Technical Memo. ERL NSSL-87, 1979, 84 pp.

6. Lemon, L. R.: New Severe Thunderstorm Radar Identification Techniques and Warning Criteria: A Preliminary Report. NOAA Technical Memo. NWS NSSFC-1, 1977, 58 pp.

7. Foster, D. C.: Aviation Hail Problems. Technical Note 37, World Meteorological Organization, Geneva, Switzerland, 1961, 160 pp.

8. Lee, J. T.; and Carpenter, D.: 1973-1977 Rough Rider Turbulence-Radar Intensity Study, Final Report. FAA Report No. FAA-RD-78-115, 1979, 22 pp.

9. Armstrong, G.; and Donaldson, R., Jr.: Plan Shear Indicator for Real-Time Doppler Radar Identification of Hazardous Storm Winds. *Journal of Applied Meteorology*, 8:376-383, 1969.

10. Burgess, D. W.; Hennington, L.; Doviak, R. J.; and Ray, P. S.: Multimoment Doppler Display for Severe Storm Identification. *Journal of Applied Meteorology*, 15:1302-1306, 1976.

11. Lee, J. T.: Applications of Doppler Weather Radar to Turbulence Measurements Which Affect Aircraft. FAA Report No. FAA-RD-77-145, 1977, 45 pp.

12. Zrnic, D. S.: Spectral Moment Estimates from Correlated Pulse Pairs. *IEEE Transactions: Aerospace and Electronics Systems*, AES-13, 1977, pp. 344-354.

13. Doviak, R. J.; Sirmans, D.; Zrnic, D.; and Walker, G. B.: Considerations for Pulse-Doppler Radar Observations of Severe Thunderstorms. *Journal of Applied Meteorology*, 17:189-205, 1978.

14. Bohne, A. R.: Radar Detection of Turbulence in Precipitation Environments. *Journal of Atmospheric Sciences*, 39:1819, 1982.

15. Zrnic, D. S.; and Lee, J. T.: Pulsed Doppler Radar Detects Weather Hazards to Aviation. *Journal of Aircraft*, 19:183, Feb. 1982.

16. National Oceanographic and Atmospheric Administration (NOAA): "NEXRAD Technical Requirements" in NEXRAD Request for Proposal SA-82-TPB-0010. U.S. Dept. of Commerce, NOAA/NWS, Aug. 1981.

17. FAA Academy: Weather and Flying Safety--Chapter 6: Thunderstorms. Mike Monroney Aeronautical Center Training Guide, Nov. 1981.

18. Eilts, M. D.; Doviak, R. J.; and Sundara-Rajan, A.: Comparison of Winds, Waves, and Turbulence as Observed by Airborne Lidar, Ground-Based Radars, and Instrumented Towers. *Radio Science*, 19(6):1511-1522, Nov.-Dec. 1984.

QUESTION: Walter Frost (FWG Associates). I noticed in one of your plots that you compare intensities using $\sigma u^2 + \sigma v^2$. Do you always compare turbulence intensities in that fashion or do you ever compare individual radial components of turbulence intensities?

ANSWER: No we use various approaches. We compare individual radial components of the Doppler radar, lidar, and tower.

FROST: When you are comparing tower lidar and Doppler data for the NASA tests, how did you collocate those sigmas?

LEE: What we did was to place these data on a grid using the Taylor hypothesis to move the tower data downwind into a location being sampled by aircraft, Doppler lidar, and Doppler radar. We did some of the early experiements with the aircraft flying right down the Doppler radar radial in the vicinity of the tower. But we did not do the experiments that were done at Huntsville. Most of our data are located on a grid matrix (0.5 km size). Lidar measurements are approximately at 500 m spacing, the Doppler radar depth is 150 m, which was averaged to 0.5 km, and, of course, in range you have a spreading out of the beam so that we felt our grid size was obtained at 0.5 km grid both vertically and horizontally at about 40 km from NSSL. The comparisons were made using those grid values.

QUESTION: Mike Tomlinson (Air Weather Service). In putting together the information you have on precipitation and then adding the Doppler spectral width and turbulence, have you tried to correlate those locations with the lightning detection systems? There is some marketing going on that says lightning information can infer turbulence information. And I'm wondering if you had an opportunity to validate or invalidate that theory.

ANSWER: We were unable to determine the relationship between lightning and turbulence. All the research studies that have been conducted in our area and in other areas indicate that there is very little in the way of correlation. Similarly, the correlation of lightning and the severity of the storm is not apparent. We have had tornadic storms in which the lightning activity has been very light. We've had extremely heavy electrical activity in storms and have had no surface manifestations of any severe weather, neither heavy rain, hail, nor high winds. We are continuing research at NSSL. We do have the radars, we have three different lightning locating systems that we are working with, the LLP, the LPAT, and one which has a very high-frequency response so that we can actually watch the strokes develop. We are trying to find out where the lightning develops. Using the dual-Doppler system to monitor the storm buildup, we are attempting to find out what flow patterns cause the separation which then ends with a discharge. But right now we see no correlation; in fact, there almost seems to be a negative correlation between the activity and turbulence--if NASA's research is an indication of all systems. I have no reason to doubt that this is not true. When an aircraft flies where there is active lightning, its flight is relatively smooth. If it goes through another area where there is hardly any lightning, the aircraft may trigger the lightning.

QUESTION: Creighton Pendarvis (SimuFlite). I've enjoyed your presentation and found it most enlightening. I'm interested in your last statement that you are now able to keep an aircraft out of a hail shaft and also out of destructive turbulence. Is there any air traffic control (ATC) facility in this country at this time that you know that has the same capability?

ANSWER: No. The NEXRAD radar system is planned for the contract to be awarded in October 1986. Their prototype radar is to be installed at Norman by March 1987. The first production radar will come in the Oklahoma City area in 1988, and then by 1989 or 1990, other units will be distributed across the United States. The Doppler radars are coming; they will be installed. A main problem, of course, in the algorithm development and interpretation, is still going to be troublesome. I think there is still going to have to be a man in the loop.

QUESTION: C. M. Tchen (City College of New York). I am interested to know whether you see a difference in the spectral density without the rain and with the rain on the same site?

ANSWER: No, we do not see the difference in convective systems we have studied. In other words we do not see any affect of rain in the layers where data were obtained.

TCHEN: The theory on the two-phase turbulence where the droplets are suspended predicts a broadening of the k^{-1} spectral distribution by the precipitation in confirmation with the Russian laser experiments. Have you measured the spectral distributions in your experiments?

LEE: Yes. It may be that if we look specifically for that effect, we might find it.

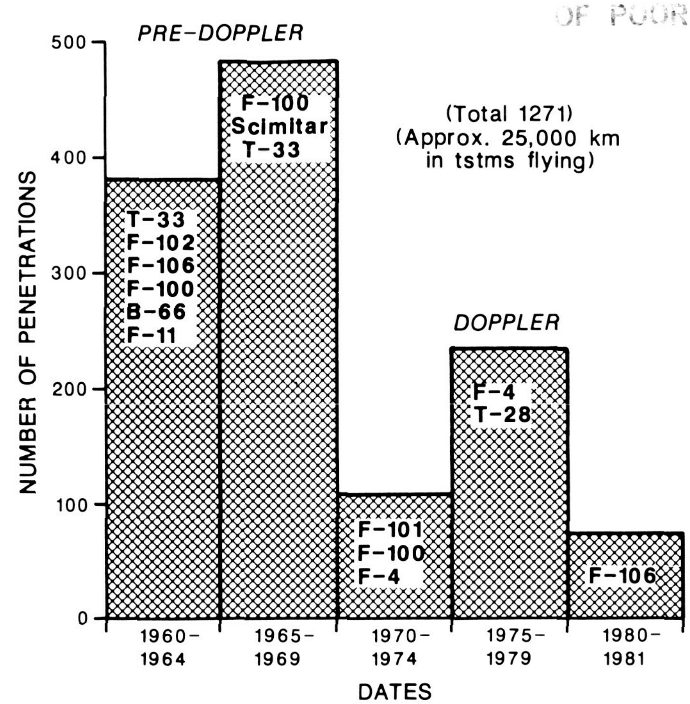

Figure 1. Number of thunderstorm penetrations made in Project Rough Rider 1960-1982 along with aircraft used in the data acquisition. Reduced numbers in 1970-1974 are results of no penetrations in 1970-1972 when emphasis was shifted to over thunderstorm flying using U-2 and RB-57F aircraft. In 1973 Doppler radar came into use and penetrations were once more initiated.

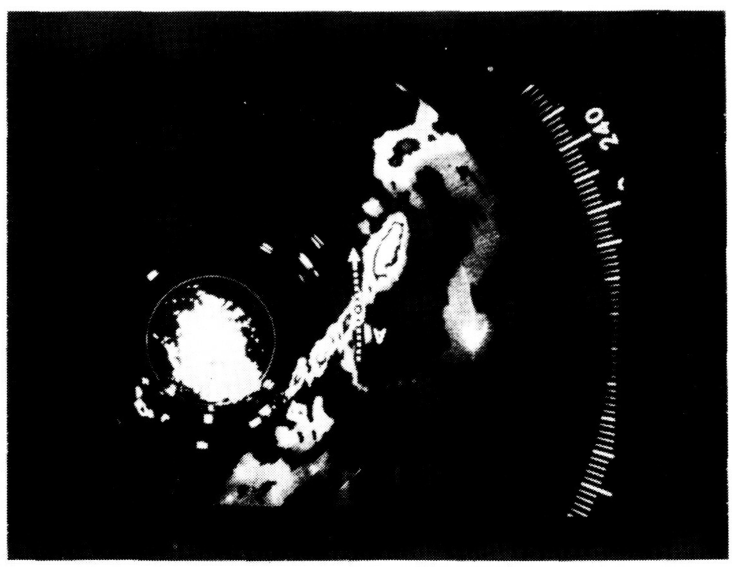

Figure 2. 16 June 1973 WSR-57 weather radar reflectivity iso-echo contour display with aircraft transponder beacons superimposed. Point "A" is the beacon return from the F-100 at 1357:25 CST; the dotted line indicates aircraft path. Range marks at 40 km intervals.

STORMS OF Ze_{max} 10^3

WHEN U_{de} EQUALS:	AND ALT IS:	0-5	6-10	11-15	16-20	21-25	26-30	30+
		TOTAL NUMBER OF OCCURRENCES = 170						
≥ 20 < 35 FT/SEC.	10-19	27(7)	4(4)	5(3)	4(1)			
	20-29	(14) 72	(12) 25	(2) 2				
	30+	7(2)	6(2)	5(1)				
≥ 35 < 50 FT/SEC.	10-19	1(1)						
	20-29	4(4)						
	30+	3(1)						
≥ 50 FT/SEC.	10-19							
	20-29							
	30+							

NUMBER OF PENETRATIONS AT

10-19 (15)	20-34	13
	35-49	4
	50+	-
20-29 (28)	20-34	28
	35-49	4
	50+	–
30+ (5)	25-34	5
	35-49	4
	50+	–

Figure 3. Distance from storm core with maximum reflectivity of $z_e = 10^3$ to 0.9×10^3 mm^6m^{-3} (30 dBZ). Turbulence is shown in three categories. Each turbulence category has penetrations divided into three altitude bands. The first indicates the number of separate occurrences while the number in parentheses indicates the number of penetrations. The occurrences are shown as a function of distance to core.

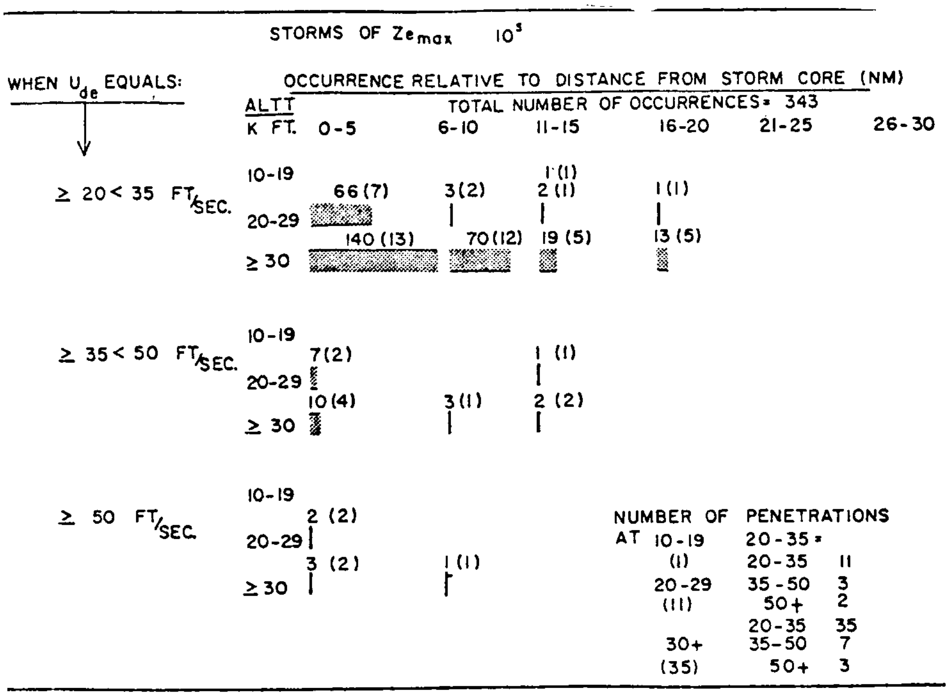

Figure 4. Distance from storm core with maximum reflectivity of 10^5 mm^6m^{-3} or more (≥50 dBZ). Turbulence is shown in three categories. Each turbulence category has penetrations divided into three altitude bands. The first indicates the number of separate occurrences while the number in parentheses indicates the number of penetrations. The occurrences are shown as a function of distance to core.

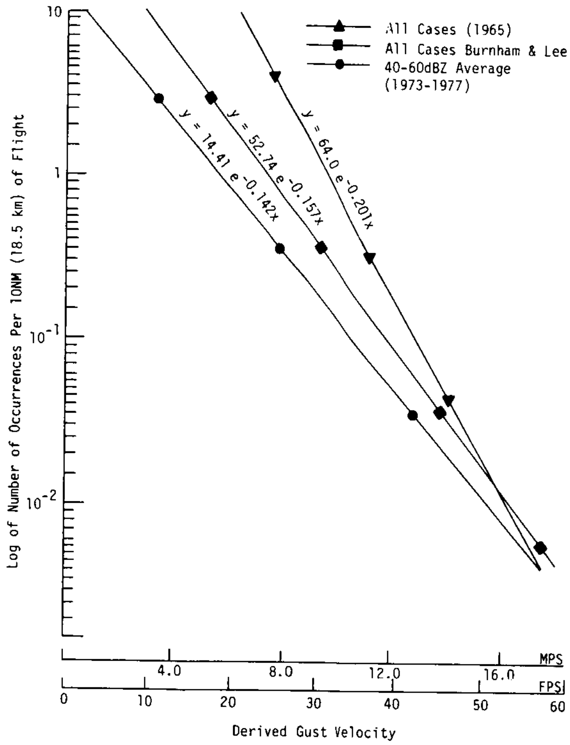

Figure 5. Frequency of turbulence encounters observed 1973-1977, as compared to observations made during the mid-1960's. Equations are exponential corresponding to the least-squares best fit for the data shown.

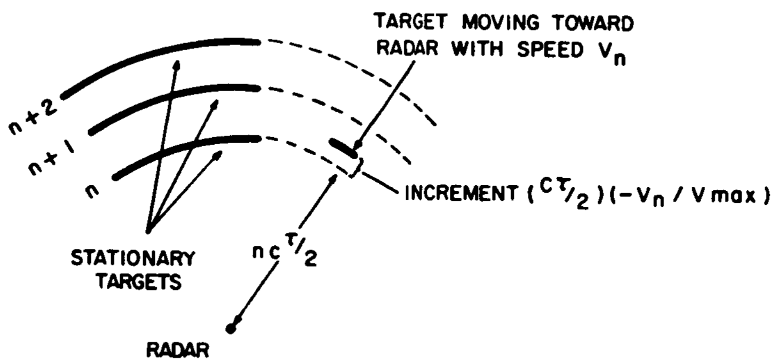

Figure 6. PSI display for stationary targets (left) and a moving target (right). The moving target is located at the same distance from the radar as the nearest stationary target (n) but is displaced from it on the PSI display by an increment proportional to its velocity.

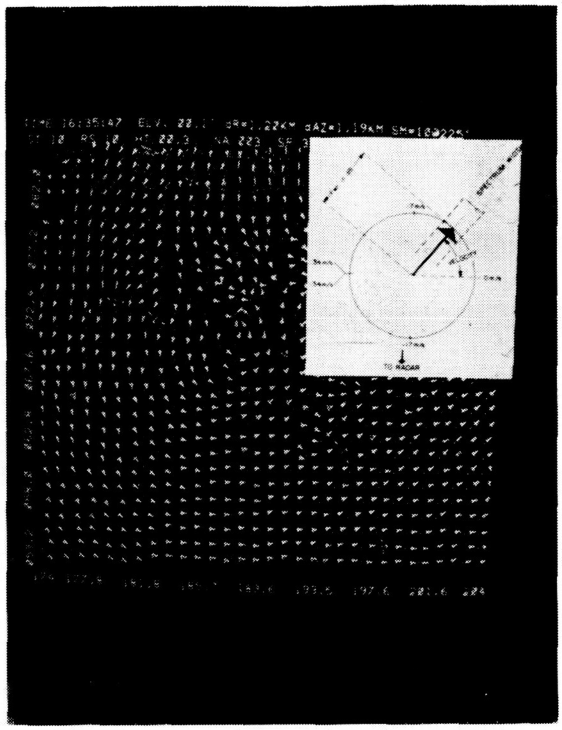

Figure 7. The multi-moment Doppler display of a mesocyclone. Each arrow contains information of the three principal Doppler spectrum moments for a resolution volume. For interpretation of arrows see insert in upper right corner (arrow length is proportional to received power, arrow direction to velocity and arrowhead size to Doppler spectrum width). Abscissa is azimuth and ordinate scale denotes range (km) from radar. Housekeeping information is at top of screen.

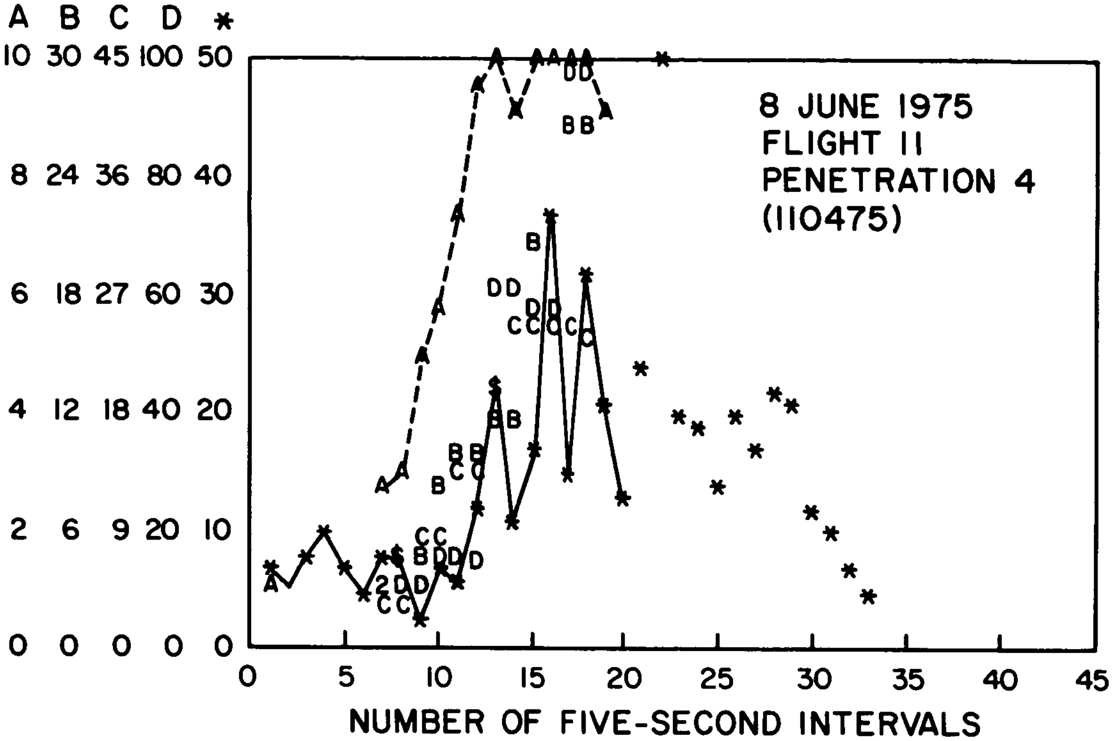

Figure 8. 8 June 1975 penetration number 4: Time (space) cross section for maximum values recorded for each five seconds of flight and corresponding Doppler radar data during penetration. Derived gust velocities in ft-1; spectrum width (A's) in ms-1; velocity gradient (B) in 1000 x s-1; Laplacian is "D." A number indicates the number of collocated data points. Dashed line connects values of spectrum width and solid line the derived gust velocities.

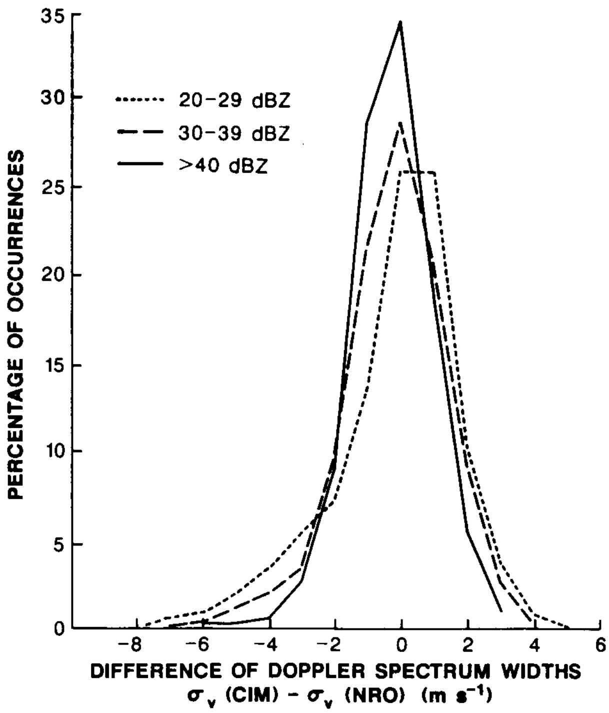

Figure 9. Comparison of spectrum widths obtained by two Doppler radars for various areas of reflectivity.

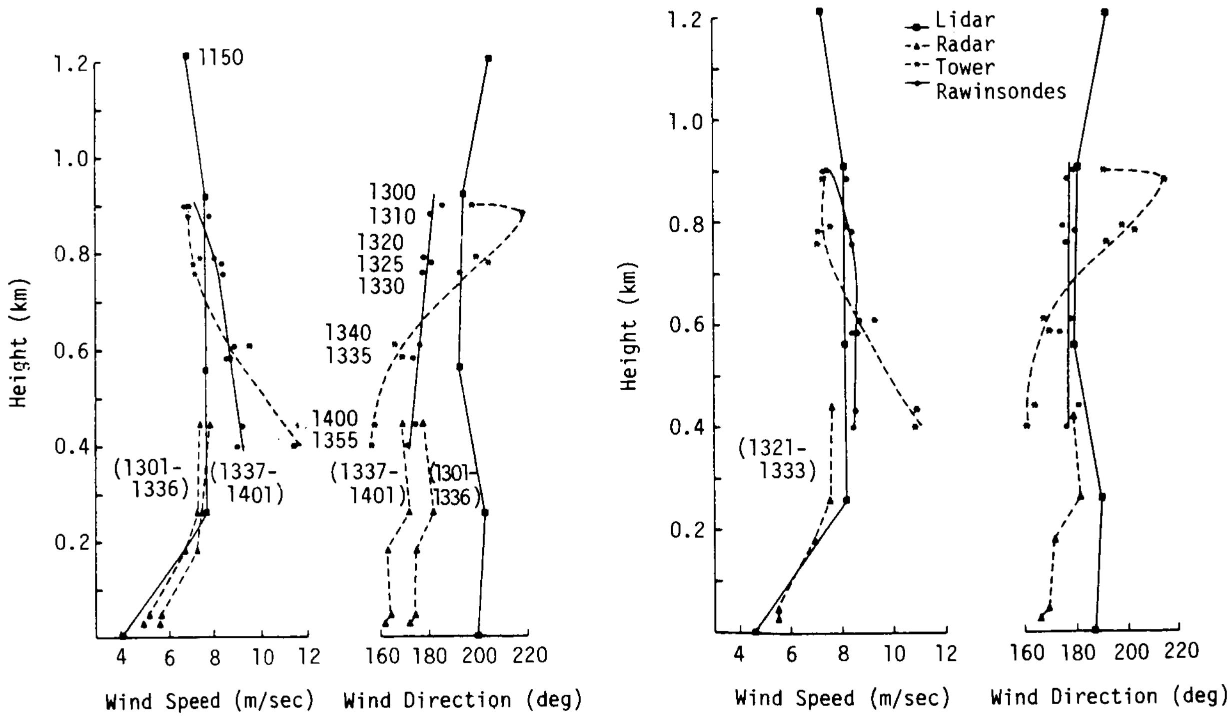

(a) Wind profiles measured by lidar, radar, tower, and rawinsondes

(b) Wind profiles measured by lidar, radar, tower, and rawinsondes adjusted to remove a time trend relative to 1330 CST. The tower profile was constructed from a 12-minute average of data from 1321-1333 CST.

Figure 10. Comparison of wind profiles.

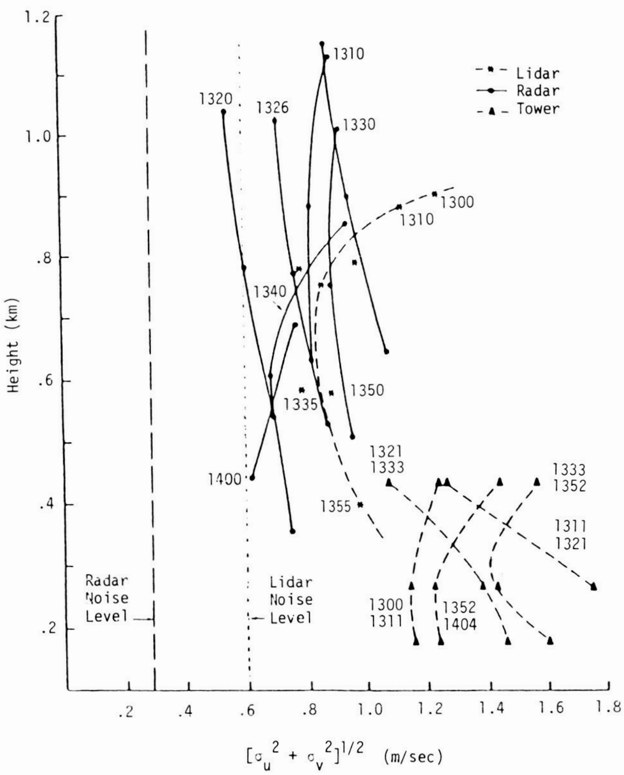

Figure 11. Standard deviation of the horizontal velocity fluctuations from lidar, radar, and tower.

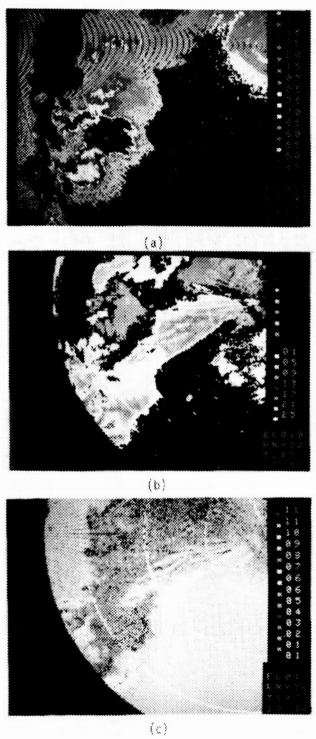

Figure 12. Doppler radar display of (a) reflectivity, (b) velocity, and (c) spectrum width of a storm south of NSSL. Note displacement of the position of areas of maximum reflectivity, maximum velocities, and maximum spectrum widths relative to each other.

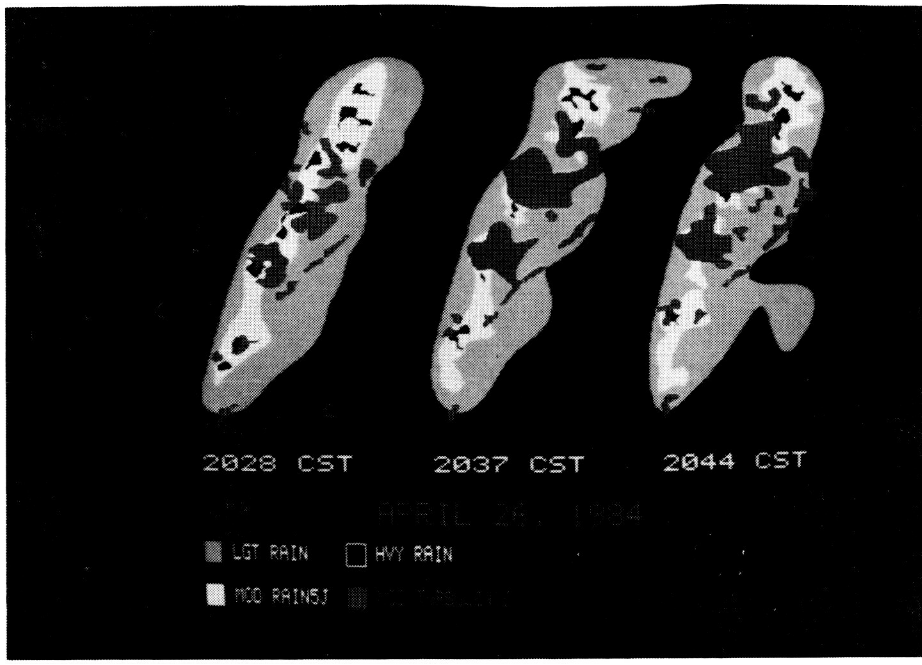

Figure 13. Storm hazard proposed NEXRAD display showing the use of a smoothing algorithm to delineate the hazard. Note time continuity of the hazards.

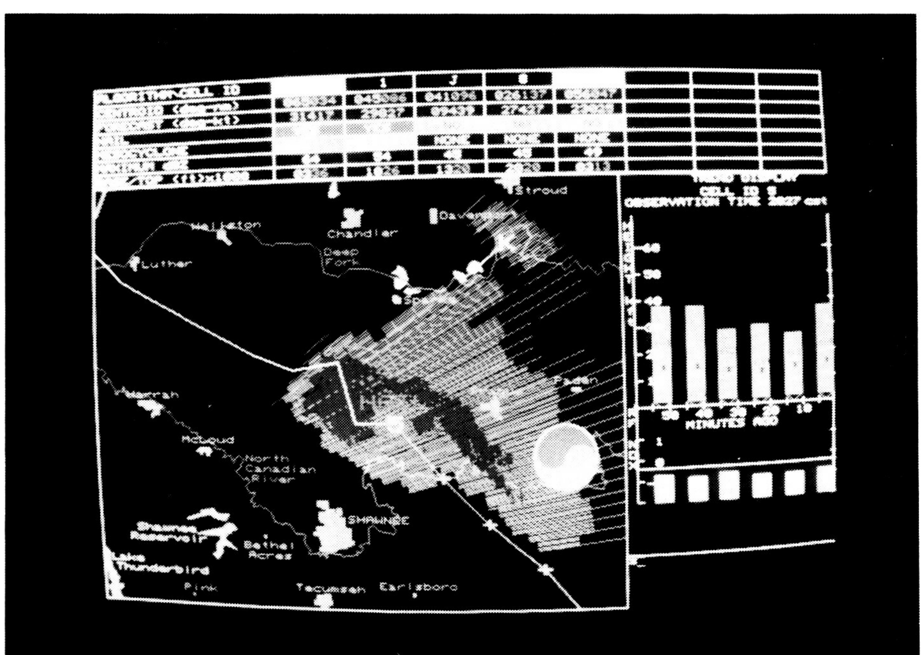

Figure 14. A second proposed type of NEXRAD display under development to provide pertinent information for a forecaster.